Catalysis Letters Vol. 105, Nos. 3–4, December 2005 (© 2005)
DOI: 10.1007/s10562-005-8696-3

Correlating low-temperature hydrogenation activity of Co/Pt(111) bimetallic surfaces to supported Co/Pt/γ-Al_2O_3 catalysts

Neetha A. Khan[a], Luis E. Murillo[a], Yuying Shu[b], and Jingguang G. Chen[b,*]

[a]*Department of Materials Science and Engineering, Center for Catalytic Science and Technology (CCST), University of Delaware, Newark, DE 19716, USA*

[b]*Department of Chemical Engineering, Center for Catalytic Science and Technology (CCST), University of Delaware, Newark, DE 19716, USA*

Received 27 June 2005; accepted 9 September 2005

The low-temperature self-hydrogenation (disproportionation) of cyclohexene was used as a probe reaction to correlate the reactivity of Co/Pt(111) bimetallic surfaces with supported Co/Pt/γ-Al_2O_3 catalysts. Temperature-programmed desorption (TPD) experiments show that cyclohexene undergoes self-hydrogenation on the ~1 ML Co/Pt(111) surface at ~219 K, which does not occur on either pure Pt(111) or a thick Co film on Pt(111). Supported catalysts with a 1:1 atomic ratio of Co:Pt were synthesized on a high surface area γ-Al_2O_3 to verify the bimetallic effect on the self-hydrogenation of cyclohexene. EXAFS experiments confirmed the presence of Co–Pt bonds in the catalyst. Using FTIR in a batch reactor configuration, the bimetallic catalyst showed a higher activity toward the self-hydrogenation of cyclohexene at room temperature than either Pt/γ-Al_2O_3 or Co/γ-Al_2O_3 catalysts. The comparison of Co/Pt(111) and Co/Pt/γ-Al_2O_3 provided an excellent example of correlating the self-hydrogenation activity of cyclohexene on bimetallic model surfaces and supported catalysts.

KEY WORDS: bimetallic catalysts; cobalt; platinum; hydrogenation; TPD; EXAFS; FTIR.

1. Introduction

Bimetallic catalysts have proven to be important materials for many catalytic applications [1–4]. Surface science investigations and density functional theory (DFT) modeling have provided a substantial amount of knowledge about the mechanisms of various chemical reactions on bimetallic surfaces [5–13]. The structural, electronic, and chemical characterization of Co/Pt bimetallic catalysts on different supports have been investigated extensively in the past by many research groups [14–18]. Specifically, the addition of Co to Pt on supported catalyst has been demonstrated to enhance the catalytic activity on CO_2 reforming of methane to syn-gas [17]. Englisch et al. have shown that Co–Pt/SiO_2 catalysts exhibit novel hydrogenation activity of crotonaldehyde toward the corresponding unsaturated aldehyde, crotyl alcohol [16].

We have previously conducted surface science studies of the novel low-temperature reaction pathways of cyclohexene on both Ni/Pt(111) and Co/Pt(111) surfaces [9,19–22]. Our surface science and DFT modeling results led to the prediction that materials such as Ni–Pt and Co–Pt would exhibit novel low-temperature activity for the hydrogenation of cyclohexene [10,20,22]. The purpose of this paper is to compare our surface science results on Co/Pt(111) with FTIR experiments on supported Co/Pt/γ-Al_2O_3 to attempt to bridge the materials and pressure gaps between surface science and catalysis studies.

* To whom correspondence should be addressed.
E-mail: jgchen@udel.edu

2. Experimental

The ultrahigh vacuum (UHV) chamber utilized for TPD and surface characterization is a two-level stainless steel chamber (base pressure of 1×10^{-10} Torr) equipped with Auger electron spectroscopy (AES), low-energy electron diffraction (LEED), and a mass spectrometer for TPD experiments, as discussed in detail in previous publications [23]. In the TPD experiments, the sample was heated with a linear heating rate of 3 K/s. The Pt single crystal sample was a (111) oriented, 1.5-mm thick Pt disk (99.999%), 10 mm in diameter. The preparation of the Co/Pt(111) bimetallic surfaces was carried out with crystal temperatures of 600 K. The Co deposition was checked for uniformity and purity on the Pt(111) surface using AES, which revealed that the surface contained less than 1% impurities during Co deposition. The coverage of the Co overlayer was estimated using the reduction of the Pt(241 eV) AES intensity after Co deposition, with the assumption that the Co overlayer grows in a layer-by-layer fashion on Pt(111) [22].

Supported Co/Pt catalysts were prepared by the incipient wetness method. The incipient wetness volume of dried γ-Al_2O_3 support was measured, and Pt and Co solutions were then prepared accordingly by adding the necessary volume of deionized water to $Pt(NH_3)_4(NO_3)_2$ and $Co(NO_3)_2{\cdot}6H_2O$ (99.999%, purchased from Alfa

1011-372X/05/1200–0233/0

Aesar) precursors, respectively. The 5 wt% Pt loading was prepared by adding the Pt solution to the γ-Al_2O_3 support drop by drop in order to keep the homogeneity of the resulting material, followed by drying at 373 K overnight and calcination at 563 K for 2 h in air. The Co/Pt/γ-Al_2O_3 catalyst was prepared by impregnating the as-prepared 5 wt% Pt/γ-Al_2O_3 in Co solutions to make a 1:1 Co to Pt atomic ratio. The Co/γ-Al_2O_3 catalyst was made with a 1.5 wt % Co loading.

The IR experiments were performed using a stainless steel IR cell consisting of BaF_2 windows, which allowed *in situ* spectroscopic studies of surface species and gas phase products in a batch reactor setup. Spectra were recorded at room temperature, with 4 cm^{-1} spectral resolution, by collecting 16 scans for gas phase spectra using a Nicolet-510 FT-IR spectrometer equipped with a DTGS detector. Powder catalysts of Co/γ-Al_2O_3, Pt/γ-Al_2O_3 and Co/Pt/γ-Al_2O_3 were pressed at $\sim$5 tons of force into 40 mg cm^{-2} self-supporting pellets. To remove water and other impurities, the sample pellets were outgassed in a dynamic vacuum (residual pressure was 2×10^{-6} Torr) at 723 K for 1 h. The samples were then reduced at the same temperature in the presence of 40 Torr hydrogen for 30 min, followed by evacuation. This procedure was repeated three times before performing the IR experiments. The vacuum manifold was equipped with two MKS-121 capacitance manometer gauges, with a pressure range from 0.1 mTorr to 1000 Torr.

Extended X-ray absorption fine structure (EXAFS) experiments were conducted on the X10-C beamline at the Brookhaven National Laboratory. Measurements were carried out in the transmission mode using a double flat crystal Si (220) monochromator and ionization chambers at room temperature. The energies of the X-ray absorption spectra were calibrated using a Pt foil (thickness of 7.5 μm) as reference. The samples were placed in a cell and heated under a hydrogen flow (130 cc min^{-1}) to 723 K with a heating rate of 10 K min^{-1}. The catalysts were maintained at this temperature for 1 h. Then, the samples were cooled down under H_2 to room temperature for the Pt L_{III}-edge EXAFS data collection. The XDAP-3.2 software was used to analyze and fit the data. Reference spectrum for the Pt–Pt bond was obtained by measuring the spectrum of a Pt foil, while FEFF8 calculations of Pt–Co interactions were used as reference for the Pt–Co contribution. The data range used in the forward k^3-weighted Fourier transform (FT) was 2.5–12.7 $Å^{-1}$. For inverse k^3-weighted FT, numerical simulations were performed between 1.5 and 3.2 Å. The interatomic distance (R), coordination number (CN), difference of the Debye–Waller factor from the reference ($\Delta\sigma^2$), and the correction of the threshold energy (ΔE^0) were treated as free parameters during the fitting procedure. The quality of the fit was estimated using the values of k^3 variance ($V_k{}^3$). Low values of variance indicate a good agreement between calculated model and experimental data.

The surface areas of supported catalysts were determined based on CO uptake by the catalyst at room temperature using Altamira Instruments (AMI-200ip). The sample catalyst of 0.1 g was loaded into a quartz reactor and reduced in H_2 at 723 K for 1 h. After cooling in Ar, pulses of CO in an Ar carrier at 30 cm^3 min^{-1} were injected at room temperature through a sample loop (535 μl) and the signal was monitored with a TCD detector. The amount of CO chemisorbed onto the catalysts and the corresponding dispersions were calculated using a stoichiometry of 1 CO molecule per surface metal atom. As summarized in table 1, the amount of CO uptake is 70.0, 89.0, and 57.3 μmol g^{-1} on Pt/γ-Al_2O_3, Co/γ-Al_2O_3, and Co/Pt/γ-Al_2O_3, respectively. The corresponding dispersion for the three catalysts is estimated to be 27.3%, 17.4%, and 22.5%, respectively.

Cyclohexene (c-C_6H_{10}) (Aldrich, 99 + % purity) was purified by successive freeze-pump-thaw cycles prior to its use in both TPD and IR experiments. The purity was verified *in situ* by mass spectrometry.

3. Results and discussion

3.1. Self-hydrogenation of cyclohexene on Co/Pt(111) surfaces

The self-hydrogenation (disproportionation) of cyclohexene (c-C_6H_{10}) produces cyclohexane (c-C_6H_{12}) and benzene (C_6H_6), with the latter also being produced from the dehydrogenation of cyclohexene. Figure 1 shows the TPD results of these two reaction products desorbing from the reaction of cyclohexene on Co/Pt(111) surfaces under UHV conditions. Cyclohexene and H_2 were also monitored in these experiments; the details of these TPD experiments have been described elsewhere [22]. On a clean Pt(111) surface and a thick Co film on Pt(111), little or no cyclohexane is produced from the self-hydrogenation of cyclohexene. However, on the $\sim$1 ML (monolayer) Co/Pt(111) surface cyclohexane is produced at a relatively low temperature (219 K). Differences in the production of benzene are also observed on the three surfaces. On a clean Pt(111) surface, benzene desorbs in a series of overlapping

Table 1
CO chemisorption results of Pt/γ-Al_2O_3, Co/Pt/γ-Al_2O_3 and Co/γ-Al_2O_3

Sample	CO uptake/μmol g^{-1}	Dispersion/%
Pt/γ-Al_2O_3(5 wt% Pt)	70.0	27.3
Co/Pt/γ-Al_2O_3(5 wt% Pt, 1.5 wt% Co, Co/Pt = 1/1)	89.0	17.4
Co/γ-Al_2O_3(1.5 wt% Co)	57.3	22.5

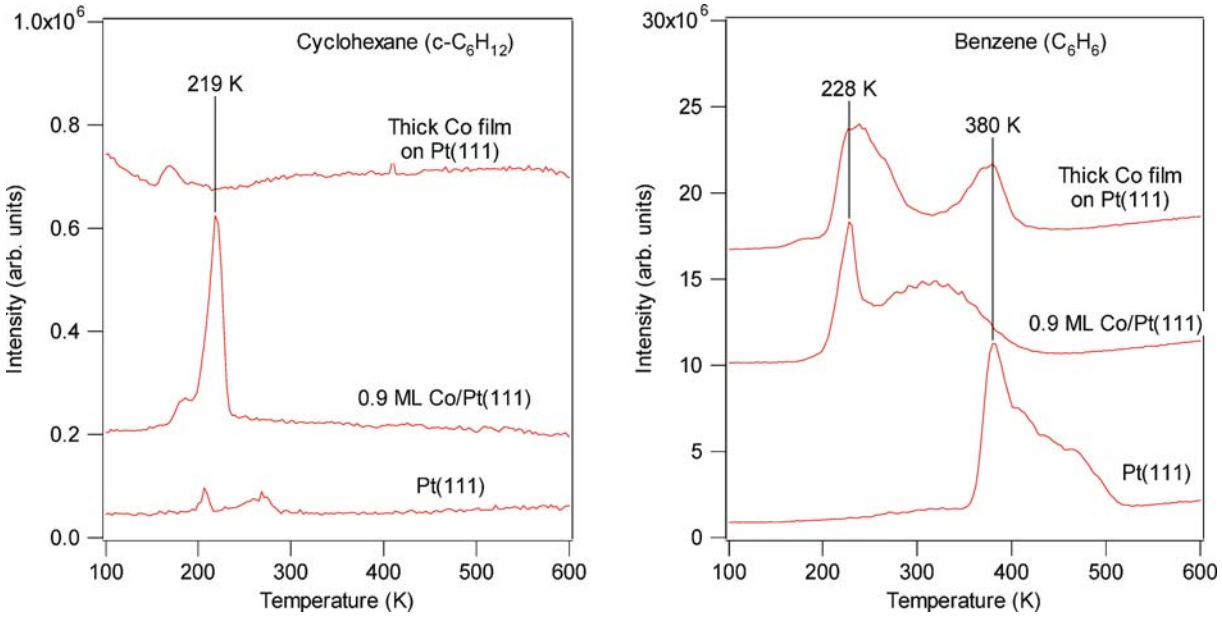

Figure 1. The self-hydrogenation product, cyclohexane (c-C_6H_{12}, 84 amu) and dehydrogenation product, benzene (C_6H_6, 78 amu) from the adsorption and reaction of cyclohexene (c-C_6H_{10}, 82 amu) on Co/Pt(111) surfaces.

peaks, starting at 380 K. On the 0.9 ML Co/Pt(111) surface, benzene desorption shifts to lower temperatures, with a sharp peak appearing at 228 K, and a broad peak at 300–400 K. Benzene desorption from the Co film on Pt(111) appears different from either the 1 ML Co/Pt(111) surface or the Pt(111) surface, with a significant amount of benzene desorbing at 228 and 380 K. The comparison of the TPD results clearly indicates that the formation of the Co/Pt bimetallic surface results in the onset of the low-temperature self-hydrogenation pathway that does not occur on either Pt(111) or a thick Co film. Lastly, the surface activities for C_6H_6 and c-C_6H_{12} on the ~1 ML Co/Pt(111) correspond to selectivities of 33 and 2%, respectively. In addition, the selectivity for decomposition pathway toward carbonaceous species on the surface was found to be 65%. The details of these calculations have been reported elsewhere [22].

3.2. *EXAFS characterization of Co/Pt/γ-Al_2O_3 and Pt/γ-Al_2O_3 catalysts*

Structural characterization of supported catalysts is often carried out by using X-ray absorption spectroscopy [24]. In particular, EXAFS is useful for the determination of the neighboring atoms about a given absorber atom and their distances by fitting the filtered data with foil or alloy references for metal–metal bond characterizations [2]. Measurements of the extended fine structure at the L_{III}-edge of platinum have been performed to confirm the presence of the Co–Pt bimetallic bonds in the supported bimetallic catalyst. Characterization of the Pt L_{III}-edge for Pt/γ-Al_2O_3 catalyst was also carried out for comparison. Table 2 shows the summary of the EXAFS results for the least-square fitting involving only a single coordination shell. The interatomic distance for the Pt–Pt bond (2.75 Å), obtained after the EXAFS fitting for the 5% Pt/γ-Al_2O_3, is at a distance slightly lower to the one found in a Pt metal foil (2.77 Å).

A comparison of the Fourier-transformed k^3-weighted EXAFS function (χ(k)) in *R*-space of filtered and fitted data for the first shell in the Pt L_{III}-edge of Co/Pt/γ-Al_2O_3 is shown in figure 2. The coordination number and interatomic distances obtained for the bimetallic Co/Pt catalyst confirms the formation of Pt–Co bonds at ~2.57 Å (table 2). This value is in accordance with the one found by Guczi et al. [18] (2.56 Å) for a bimetallic catalyst on alumina with a Co/Pt atomic ratio of 9. The interatomic distance for Pt–Pt in the bimetallic sample decreases to 2.74 Å from the expected value in a Pt metal foil (2.77 Å). This change in the interatomic Pt–Pt distances is a function of the concentration of Pt in the bimetallic nanoparticles, as was demonstrated in a study of crystallographic structure of cobalt thin films deposited on Pt(111) by Thiele et al. [25].

Table 2
Results of Pt LIII-edge EXAFS fitting on Pt/γ-Al_2O_3 and Co/Pt/γ-Al_2O_3

Sample	Shell	CN	*R*/Å	$\Delta\sigma^2$/ 10^{-3} Å^2	ΔE^0/eV	V_{fit}
5 wt%Pt/γ-Al_2O_3	Pt–Pt	9.2	2.75	2.87	2.7	0.65
Co/Pt/γ-Al_2O_3	Pt–Pt	6.6	2.74	1.7	10.7	0.42
	Pt–Co	2.7	2.57	7.5	8.4	

R-space and k^3 weighting; $\Delta k = 2.9/12.1$ Å^{-1}; $\Delta R = 0/4$ Å.

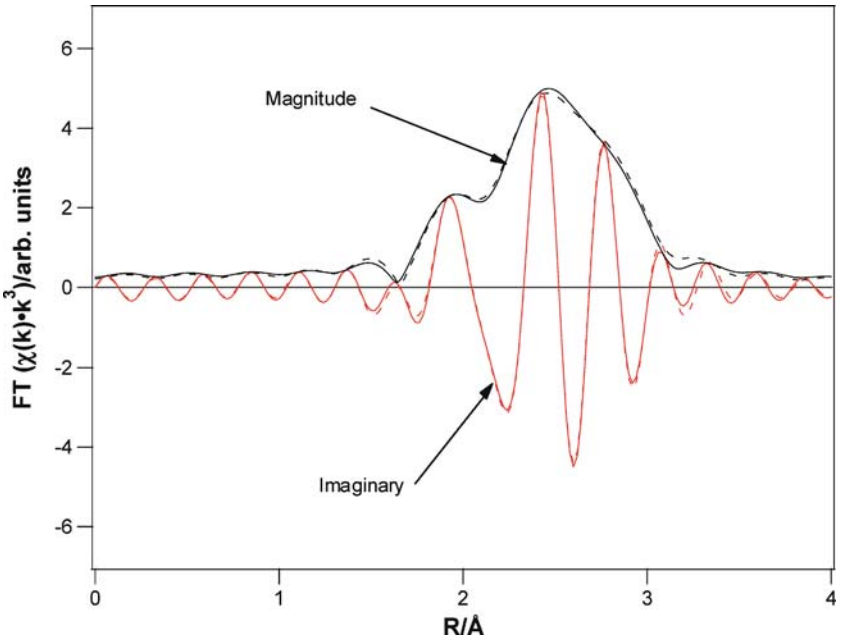

Figure 2. Fourier-transformed (imaginary and magnitude) k^3-weighted EXAFS function ($\chi(k)$) of Pt L_{III}-edge of Co/Pt/γ-Al_2O_3, filtered (dashed) and fitted (solid) EXAFS curves.

3.3. *FTIR of cyclohexene reaction pathways on Co/Pt/γ-Al_2O_3 catalysts*

In the FTIR experiments, the reaction products were monitored at room temperature using gas phase spectra, taken every 150 s during the reaction. The IR cell was filled with 10 Torr cyclohexene and gas-phase IR spectra were recorded at room temperature. The concentrations of the three main species cyclohexene, cyclohexane, and benzene were determined using the intensities of the vibrational features at 1139 cm^{-1} (ωCH_2 rock) [26], 1458 cm^{-1} (–CH_2 deformation) [27], and 1810 cm^{-1} (overtone of the C–C stretching mode at 993 cm^{-1}) [28], respectively. However, the 1458 cm^{-1} feature of cyclohexane overlaps with a cyclohexene feature at 1455 cm^{-1} (–CH_2 deformation) [28] and a benzene feature at 1488 cm^{-1} (ring stretching and deformation) [27]. Figure 3 shows the gas-phase changes in intensity of these features during the reaction of cyclohexene over the Co/Pt/γ-Al_2O_3 catalyst at three different reaction times. After 150 s of reaction, the onset of benzene is observed at 1810 cm^{-1} and the presence of cyclohexane is detected at ~1458 cm^{-1}. The formation of both benzene and cyclohexane is more evident after 2250 s. After ~4500 s, the absence of the characteristic band of cyclohexene (~1139 cm^{-1}) suggests that the reaction is complete. In order to more accurately account for cyclohexane production, the contributions from cyclohexene and benzene were subtracted from the intensity of the 1458 cm^{-1} feature as shown below.

First, the intensity ratios between the overlapping peak and the non-overlapping peaks of cyclohexene and benzene were calculated (K_1 and K_2, respectively).

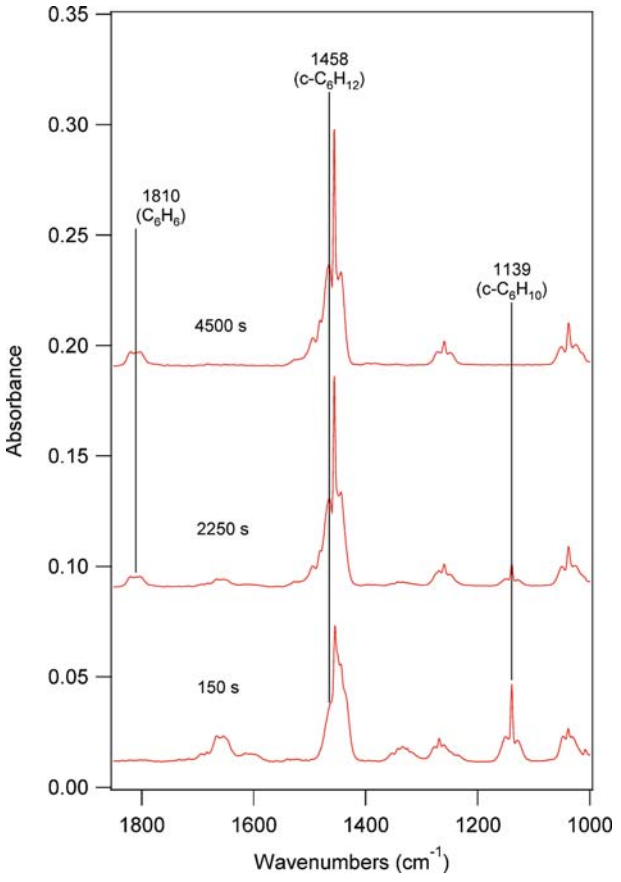

Figure 3. Gas-phase FTIR spectrum during the reaction of cyclohexene over Co/Pt/γ-Al_2O_3 catalysts at room temperature at three different reaction times.

The IR cell was filled with cyclohexene and benzene separately, without any catalyst. From the gas phase IR spectra of the pure species the following ratios of K_1 for cyclohexene and K_2 for benzene were determined:

$$K_1 = \frac{S_{1139}(\text{c-}C_6H_{10})}{S_{1455}(\text{c-}C_6H_{10})} = 0.32 \qquad K_2 = \frac{S_{1810}(\text{c-}C_6H_6)}{S_{1488}(\text{c-}C_6H_6)} = 0.38$$

These ratios were used to subtract out the cyclohexene and benzene contributions to the peak at 1458 cm^{-1} in the reaction mixture in the following manner.

$$S_{1458}(\text{c-}C_6H_{12}) = S_{1455}(\text{total}) - \left(\frac{S_{1139}(\text{c-}C_6H_{10})}{K_1}\right) - \left(\frac{S_{1810}(\text{c-}C_6H_6)}{K_2}\right)$$

The IR intensity of cyclohexene, benzene, and cyclohexane were calibrated to the number of molecules by measuring the intensities of the corresponding features at various concentrations of cyclohexene, benzene, and cyclohexane, respectively. These values were then normalized to the number of surface sites based on the dispersion values in table 1. The kinetics of cyclohexene self-hydrogenation on the Co/Pt/γ-Al_2O_3 catalyst is shown in figure 4. Figures 3 and 4 demonstrate that the Co/Pt/γ-Al_2O_3 catalyst is active at room temperature for the production of both cyclohexane and benzene. The ratio of cyclohexane to benzene production is approximately 1.8, consistent with the self-hydrogenation reaction pathway, which should result in a cyclohexane/benzene ratio of 2.0.

Figure 5 compares the rates of cyclohexane and benzene formation, in units of number of molecules per surface metal atoms on the catalyst, over Pt/γ-Al_2O_3, Co/γ-Al_2O_3, and Co/Pt/γ-Al_2O_3 catalysts. The Co/Pt/γ-Al_2O_3 catalysts clearly show a higher self-hydrogenation rate at room temperature than either Co/γ-Al_2O_3 or Pt/γ-Al_2O_3. In order to quantify the difference between the self-hydrogenation rates on the three catalysts, first-order kinetics was assumed for the production of cyclohexane and benzene. The solid lines in figure 5 represent the fittings using first-order kinetics. The rate constants were calculated to be 6.4×10^{-4}, 2.5×10^{-4}, and 0 s^{-1} for Co/Pt/γ-Al_2O_3, Pt/γ-Al_2O_3, and Co/γ-Al_2O_3 catalysts respectively.

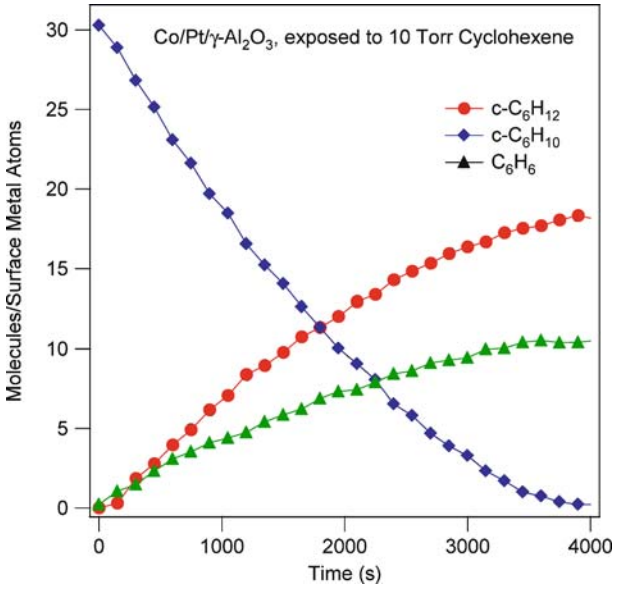

Figure 4. Comparison of the rates of cyclohexene consumption and cyclohexane and benzene production over the Co/Pt/γ-Al_2O_3 catalysts at room temperature.

3.4. Possible origin of self-hydrogenation activity

The TPD and FTIR results indicate that the Co/Pt(111) bimetallic surface and the supported Co/Pt/γ-Al_2O_3 catalyst are more active than the corresponding monometallic surfaces and catalysts. As discussed in our previous surface science [22] and DFT modeling [10], atomic hydrogen bonds more weakly on the Co/Pt(111) surface than on either pure Pt(111) or Co(0001). The weaker metal hydrogen bond on the Co/Pt(111) bimetallic surface is most likely responsible for its low-temperature hydrogenation activity.

In addition, DFT modeling from both our group [10] and others [29] indicates that the preferred structure of the Co/Pt(111) surface, at a monolayer coverage, is the Pt–Co–Pt(111) structure with the monolayer Co occupying between the first and second layers of Pt. This Pt–Co–Pt 'sandwich' structure is stable under reducing conditions, such as in vacuum and hydrogen environment [10,13]. In the current study the Co/Pt(111) surface and the supported Co/Pt/γ-Al_2O_3 catalyst are both prepared under reducing conditions. It is likely that the model surface and supported catalyst are both characterized with Co atoms occupying the subsurface sites underneath the first layer of Pt, leading to the very good agreement in the reactivity between model surfaces and supported catalysts.

4. Conclusions

In this paper we have shown a correlation between the low-temperature self-hydrogenation of cyclohexene on Co/Pt(111) surfaces and on Co/Pt/γ-Al_2O_3 catalysts. Unlike the pure metal surfaces, the ~1 ML Co/Pt(111) surface leads to the low-temperature self-hydrogenation of cyclohexene. Supported Co/Pt catalysts were synthesized and characterized to bridge the materials and pressure gaps between surface science and catalysis. EXAFS results show that the Co/Pt/γ-Al_2O_3 catalyst contains Co–Pt bonds, confirming the formation of bimetallic in the supported catalysts. The FTIR results reveal that the Co/Pt/γ-Al_2O_3 bimetallic catalyst shows a higher activity toward the self-hydrogenation of cyclohexene reaction

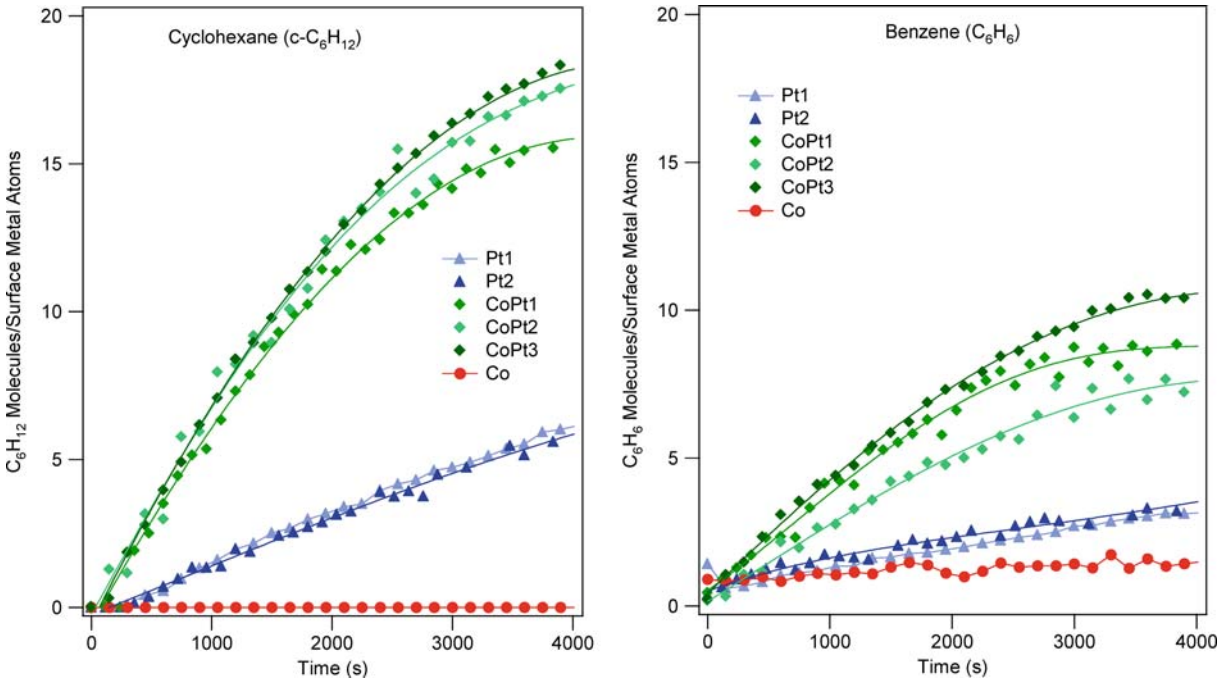

Figure 5. FTIR measurements of cyclohexane and benzene production from the reaction of cyclohexene over Pt/γ-Al_2O_3, Co/Pt/γ-Al_2O_3, and Co/γ-Al_2O_3 catalysts at room temperature. The designation of CoPt1, CoPt2, and CoPt3 represents multiple measurements, each with fresh bimetallic CoPt catalysts, as well as, Pt1 and Pt2, each with fresh Pt catalysts, to assure the reproducibility of the reactivities. The solid lines represent fittings using first-order kinetics.

pathway than either Co/γ-Al_2O_3 or Pt/γ-Al_2O_3 catalysts, demonstrating a good agreement between model surfaces and supported bimetallic catalysts.

Acknowledgments

The authors would like to acknowledge the Department of Energy, Office of Basic Energy Sciences (Grant# DE-FG02-00ER15014) for funding. Y. Shu would like to acknowledge partial support from NSF for an international collaboration grant (NSF-INT-0321942). The authors would also like to acknowledge Dr. V. Schwartz for help with the Co/Pt/γ-Al_2O_3 catalyst preparation and EXAFS analysis. We also acknowledge Exxon-Mobil for providing the beam time on the X10-C beamline at NSLS-BNL for EXAFS measurements.

References

[1] J.H. Sinfelt, Accounts Chem. Res. 10 (1977) 15.
[2] J.H. Sinfelt, *Bimetallic Catalysts: Discoveries, Concepts, and Applications* (John Wiley and Sons, New York, 1983).
[3] N.M. Markovic and P.N. Ross, Electrochim. Acta 45 (2000) 4101.
[4] N. Tsubaki, S.L. Sun and K. Fujimoto, J. Catal. 199 (2001) 236.
[5] B. Hammer and J.K. Nørskov, Surf. Sci. 343 (1995) 211.
[6] D.W. Goodman, J. Phys. Chem. 100 (1996) 13090.
[7] B. Hammer and J.K. Nørskov, Adv. Catal. 45 (2000) 71.
[8] N.M. Markovic and P.N. Ross, Surf. Sci. Rep. 45 (2002) 121.
[9] J.R. Kitchin, N.A. Khan, M.A. Barteau, J.G. Chen, B. Yakshinksiy and T.E. Madey, Surf. Sci. 544 (2003) 295.
[10] J.R. Kitchin, J.K. Nørskov, M.A. Barteau and J.G. Chen, J. Chem. Phys. 120 (2004) 10240.
[11] J.R. Kitchin, J.K. Nørskov, M.A. Barteau and J.G. Chen, Phys. Rev. Lett. 93 (2004).
[12] Y. Xu, A.V. Ruban and M. Mavrikakis, J. Am. Chem. Soc. 126 (2004) 4717.
[13] J. Greeley and M. Mavrikakis, Nat. Mater. 3 (2004) 810.
[14] D. Schanke, S. Vada, E.A. Blekkan, A.M. Hilmen, A. Hoff and A. Holmen, J. Catal. 156 (1995) 85.
[15] B. Moraweck, R. Frety, G. Pecchi, M. Morales and P. Reyes, Catal. Lett. 43 (1997) 85.
[16] M. Englisch, V.S. Ranade and J.A. Lercher, J. Mol. Catal. A 121 (1997) 69.
[17] S. Tang, J. Lin and K.L. Tan, Surf. Interface Anal. 28 (1999) 155.
[18] L. Guczi, Top. Catal. 20 (2002) 129.
[19] H.H. Hwu, J. Eng Jr. and J.G. Chen, J. Am. Chem. Soc. 124 (2002) 702.
[20] N.A. Khan, J.R. Kitchin, V. Schwartz, L.E. Murillo, K.M. Bulanin and J.G. Chen, in: *Nanotechnology in Catalysis*, eds. S.H.B. Zhou and G.A. Somorjai (New York, 2003).
[21] N.A. Khan, M.B. Zellner, L.E. Murillo and J.G. Chen, Catal. Lett. 95 (2004) 1.
[22] N.A. Khan, L.E. Murillo and J.G. Chen, J. Phys. Chem. B 108 (2004) 15748.
[23] N.A. Khan, M.B. Zellner and J.G. Chen, Surf. Sci. 556 (2004) 87.
[24] J.W. Niemantsverdriet, *Spectroscopy in Catalysis* (Wiley-VCH, Weinheim (Germany), 2000).
[25] J. Thiele, R. Belkhou, H. Bulou, O. Heckmann, H. Magnan, P. LeFevre, D. Chandesris and C. Guillot, Surf. Sci. 384 (1997) 120.
[26] A.V. Kiselev and V.I. Lygin, *Infrared Spectra of Surface Compounds* (John Wiley and Sons, New York, 1975).
[27] T. Shimanouchi, *Tables of Molecular Vibrational Frequencies Consolidated*, Vol. I, National Bureau of Standards, 1972.
[28] N.B. Colthup, L.H. Daly and S.E. Wiberley, *Introduction to Infrared and Raman Spectroscopy* (Academic Press, Inc., San Diego, 1990).
[29] A.V. Ruban, H.L. Skriver and J.K. Nørskov, Phys. Rev. B 59 (1999) 15990.